3D Laser Scanner Scenes Registration Using Artificial Bee colony optimization Based Heat Kernel Signature

Bayumy A. B. Youssef
Informatics institute, The City for Scientific Research and Technology Applications Alexandria, Egypt.

Abstract

This paper proposes an algorithm for 3D laser scanner scenes registration. The registration will preformed using artificial bee colony (ABC) optimization as objective function solver and heat kernel signature as registration parameter. The property of the scanner's position was used as a pivot for rotation R and translation T the target scene to maximize the proposed objective function. The function that is used is measuring how many points of target cloud Q do match with the corresponding points of reference cloud P. The objective is to maximize the number of matched points. The initial target's position was devoted to compare both the accuracy and the computation time of the algorithm. The three realistic data sets were used for validating the algorithm. They were collected from Babylon Fortress (Cairo-Egypt), sphinx (Giza-Egypt) and the site of our academy (Alexandria-Egypt). The results demonstrate well-posed alignment for all data sets.

Key words: 3D Laser scanner, Registration, Artificial Bee colony, ABC, optimization, Heat kernel signature

1. Introduction

Nowadays 3D laser scanner has a big contribution in many fields such as reverse engineering, Archeological documentation and preservation, mining, agriculture, cities virtual tour. 3D laser scenes persistently need registration to complete the all plateau fast and accurately. Large number of algorithms have been developed to fulfill these targets. 3D laser scanner scenes registration is persistently needed in the all of laser scanner applications. Recently, many research has been devoted to enhance the 3D registration processes both accuracy and computational time. Torre et. al.[1] have introduced a new algorithm of registration based on a purpose-designed similarity measure. Bayumy et. al. [2] proposed an efficient registration algorithm using wavelet features. Meierhold et. al. [3] introduced an automatic feature matching between digital images and 2D representations of a 3D laser scanner's point cloud. Torre et. al. [4] used an alternative 3D shape representation to preform registration. Wang et. al. [5] have done an automatic registration of mobile lidar and spherical panoramas. Abbas et. al. [6] have made an investigation into the registration of lidar intensity data and aerial images using the sift approach. Ebadat et. al. [7] developed an automatic registration of optical imagery with 3D lidar data using local combined mutual information. Yamany and Farag [8] used the surface signatures for 3D registration. This paper proposes an algorithm for 3D laser scanner scenes registration. The registration will preformed using artificial bee colony (ABC) optimization as objective function solver and heat kernel signature as registration parameter. ABC algorithm is inspired by the behavior of honeybee swarms [9]. ABC is robustness, fast convergence and flexibility. In addition, it has fewer controlled parameters. Heat kernel signature describes intrinsic local shape based on diffusion scale-space analysis [10]. It analogies the heat diffusion equation. It is introduced as a parameter of registration that is invariant with object translation or rotation. Jihua et. al. [11] offered an automatic multi-view registration of unordered range scans without feature extraction. Jun Xiea et. al. [12] proposed an algorithm for fine registration of 3D point clouds fusing structural and photometric information using an RGB-D camera. Dirk Holz and Sven Behnke. [13] presented a registration of non-uniform density 3D laser scans for mapping with micro aerial vehicles.

2. Methodology

The algorithm is composed of the following basic procedures:

A. Initialization
   1. 3D-Laser scene representation in 2D scheme (reference and target scenes) to mesh the data set of them
   2. Heat kernel signature calculations for the meshed data set

B. Iterative procedure using (ABC) optimization method to converge to maximize the proposed objective function that is a function of transformation vector (R_x, R_y, R_z, T_x, T_y, T_z). where R,T represent rotation and translation , and x, y, z are spatial coordinates
   1. Generate the transform vector using the criteria of ABC
   2. Calculate the proposed objective function

C. Repeat step B until the maximization is acquired.

2.1. Point Cloud Measure

The points cloud has been acquired using terrestrial Laser-Imaging-System I-SiTe 4400 that is a combined Laser-Scanner survey and panoramic digital photography instrument as shown in Fig. 1. The panoramic digital camera does not concerned in this work. Laser-Scanner survey has a maximum field of view of 80° in vertical and 360° in horizontal direction. Each scene is acquired by the density of 2.5 million points can be acquired at 4000 points/second. Figure 2 shows some samples measured by this laser scanner.

Fig. 1: The Laser-Imaging-System I-SiTe 4400

2.2. Meshing of Point cloud

In order to calculate the heat kernel signature, the point cloud must be meshed. The method, which the laser utilizes to scan the point cloud, is exploited to perform the meshing. The scanner acquires the point cloud in columns and rows arrange with resolution $\Delta\theta$ in column direction and $\Delta\varphi$ in row direction. The laser scanner can covered each column from θ_{min} to θ_{max} and each row from φ_{min} to φ_{max} as shown in Fig. 2. 3D laser scanner provide for each point p the polar coordinates (θ, φ) and other attributions such as x, y, z coordinates. With this provision, the 2D representation is attained in (θ, φ) axes aver virtual image plane as shown in Fig. 2. Also now, we have a structured rectangular mesh as shown in Fig. 3[3]. Finally, the axes (θ, φ) are swapped to 3D axes (x, y, z) as shown in Fig.4.

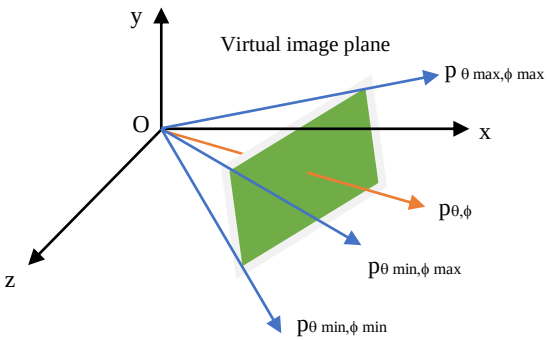

Fig 2. Definition of the coordinate scanner system

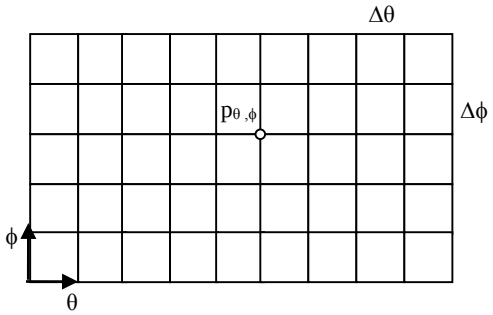

Fig. 3: representation 3D laser scanner range image as 2D image virtual image plane

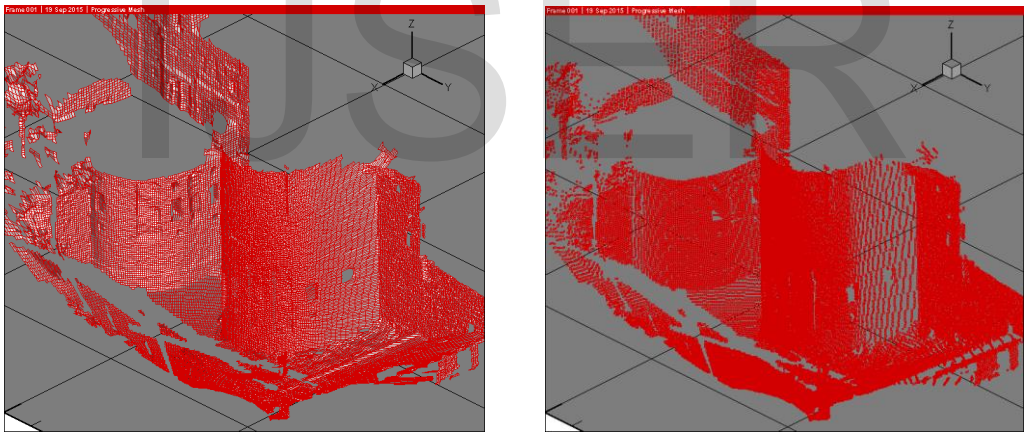

Meshed scene point cloud

Fig. 4: represents mashed 3D laser scanner scene versus its point cloud

2.3. Heat kernel calculation[10]

Heat kernel signature (*H*) calculation is based on the heat diffusion equation, which yields to:

$$\frac{\partial u(x,t)}{\partial t} = \Delta u(x,t) \quad 1$$

Where, Δ denotes the positive semi-definite Laplace Beltrami operator, *u(x,t)* denotes the solution vector, *x* is the spatial domain, and t time domain

H is calculated supposing that $u(x,0) = u(x)$ where all the heat energy is concentrated in a point *x* at *t=0*. Then amount of heat energy remains at the same point x for time t > 0 is considered *H*. Then

$$H = K_t(x, x) \quad 2$$

Where K_t is heat kernel which can be considered the amount of heat transferred from point *x* with given a unit heat source to point *y* in time *t*.

$$K_t(x, y) = \sum_{i=1}^{\infty} e^{-\lambda_i t}\, \phi_i(x)\phi_i(y) \quad 3$$

Where, $\lambda_1, \lambda_{21}, \lambda_3, \ldots\ldots\ldots\ldots \geq 0$ are eigenvalues and $\phi_1, \phi_2, \phi_3, \ldots\ldots$ are the corresponding Eigen functions of the Laplace-Beltrami operator, satisfying $\Delta\phi_i = \lambda_i\, \phi_i$

H can be approximated the by using only 300 eigenvalues and eigenvectors. It then yields to*:*

$$K_t(x, x) = \sum_{i=1}^{300} e^{-\lambda t}\Phi_i(x)\Phi_i(x) \quad 4$$

2.4. Artificial Bee Colony (ABC) Algorithm[14,15]

ABC consists of four main phases: First initialization phase where the sites, which have a food, are randomly generated by scouts. Second employees phase where are recruited to fly to these sites to search about new food sites within their neighbors and return to do the waggle dance. Third onlooker bees phase whereas see the waggle dance and evaluate the fitness of sites, and then randomly select the site that has a higher quantity of food. After that, onlooker bees randomly search in this site's neighbors. The food quantity of a site is evaluated by its fitness compared with the fitness of all sites. Finally scout phase if the site's fitness doesn't improve with running time, the solutions will be abandoned by scout. Then, the scouts start to randomly search the new solutions.

The initial sites of food are randomly produced via the expression

$$S_M = L + random(1,0) * (U - L) \quad 5$$

Where *S* is site of food that has M dimension, L, U are the upper and lower bound of the solution space of objective function.

The employed Bee, which are recurred to search new sites, which are neighboured to S, is determined by the following equation

$$V_{Mi} = S_{Mi} + random(-1,1) * (S_{Mi} - S_{Mk}) \quad 6$$

Where *V* the vector of search new sites which are neighboured to *S*, *i* is a randomly selected site of food, *k* is a randomly selected the neighbours site of food *i*.

Onlooker Bee can evaluate site's food quantity *k* with respect to the other sites using the following formula

$$E_k = \frac{f_k}{\sum_{i=1}^{M} f_i} \quad 7$$

Where *E* is evaluation criteria, *f* is the fitness.

Onlooker bees search the neighbourhood of food source according to equation 6

2.5. Fitness Function

ABC uses the function (*f*) which is measuring how many points of target cloud Q do match with the corresponding points of reference cloud P. The match occurs when the difference of heat kernel signature property realizes certain threshold δ. The resulting the number of matched points rely on the position of target with respect to the reference. This position changes by changing the parameters of the transformation matrix which are $T\ (T_x,T_y,T_z)$ and rotation $R\ (R_x,R_y,R_z)$. The objective is to maximize function (*f*). Then the objective function yields to:

$$Maximize\ f(T,R) = Count\big(P \cap Q\ :\ \big(H(p_i) - H(q_j)\big) < \delta\big) \quad i \forall P\ ,\ \ j \forall Q$$

Where p_i is a point of P, q_j is a point of Q and H is the heat kernel signature.

3. Results and discussions

3.1. Datasets

The proposed algorithm was tested using three data sets that were acquired using 3D laser scanner (I-site) and are available in our institute. The all of three are realistic datasets where were collected from Babylon Fortress (Cairo-Egypt), sphinx (Giza-Egypt) and the site of our academy (Alexandria-Egypt) as shown in Fig. 5.

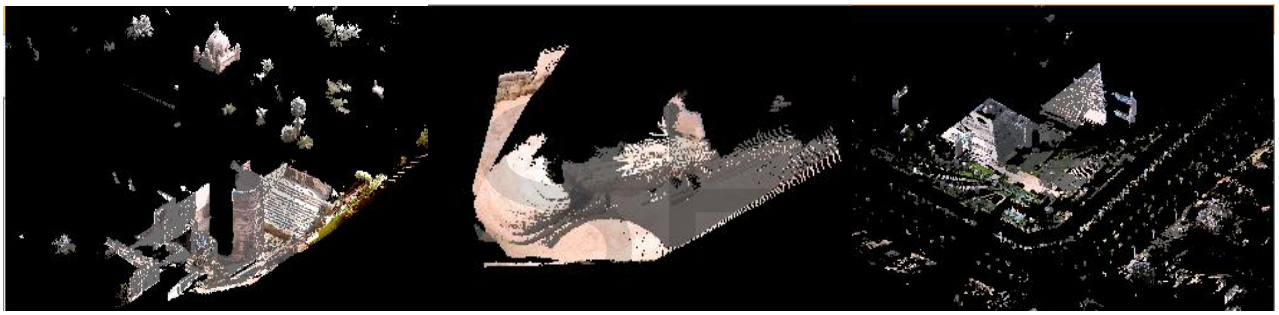

Fig. 5: Realistic datasets of Babylon Fortress (Cairo-Egypt), sphinx (Giza-Egypt) and the site of our academy (Alexandria-Egypt)

3.2. Heat kernel signature distribution

Fig. 6 shows the distribution of heat kernel signature on the reference and target scenes of Babylon Fortress with 300 eigenvalues and eigenvectors. It shows also well-posed similarity between the similar geometry shapes in both reference and target.

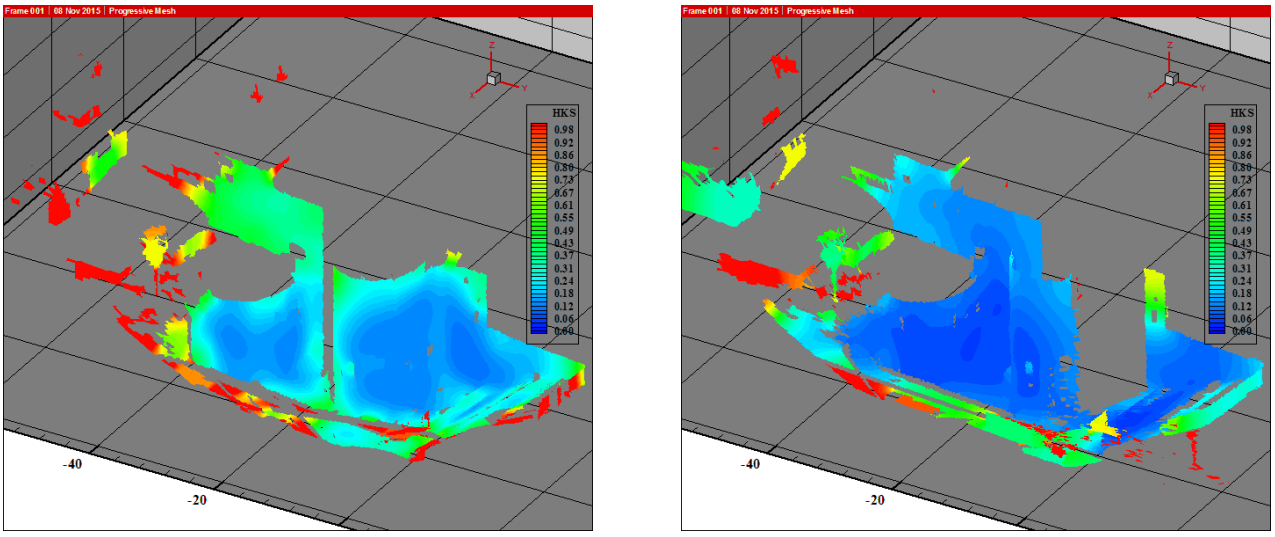

Fig. 6. Heat kernel signature distribution on the reference and target scenes of Babylon Fortress with 300 eigenvalues and eigenvectors.

3.3. Registration alignment accuracy and computation time

The data set of Babylon Fortress with six different target's position were devoted to compare the accuracy and the computation time. If the exact solution vector is Sol={R_{xo}, R_{yo}, R_{zo}, T_{xo}, T_{yo}, T_{zo}} then the six target's position are {Sol+1}, {Sol+3},{Sol+5}, {Sol+10}, {Sol+20}, and {Sol+30} which are respectively denoted by E01, E03, E05, E10, E20, and E30.

As shown in Fig's (7-12), the results demonstrate well-posed alignment for all six cases E01, E03, E05, E10, E20, and E30.

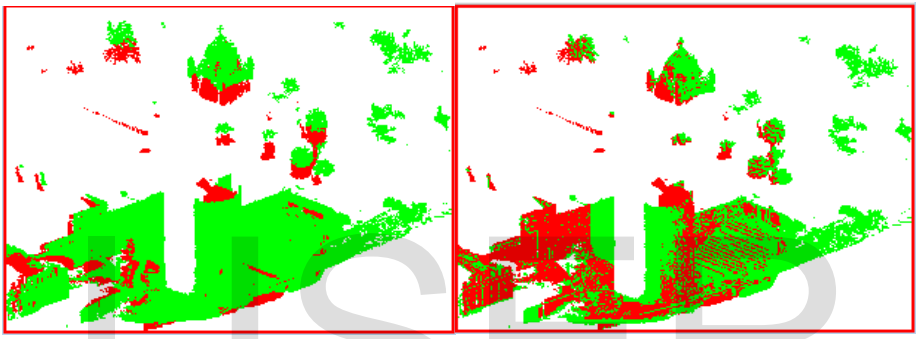

Fig. 7: the alignment of case E01

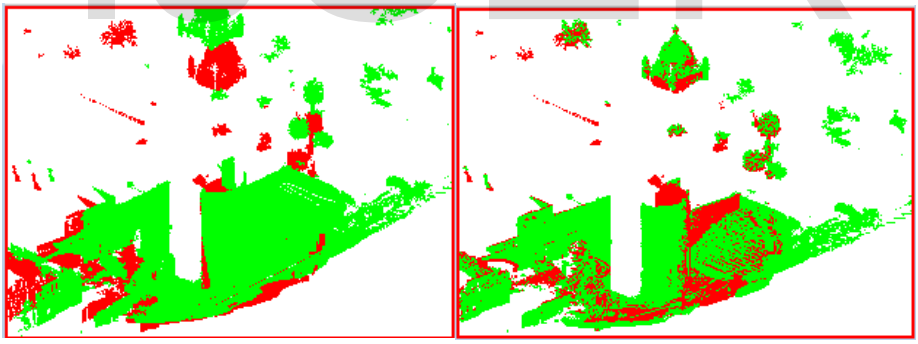

Fig. 8: the alignment of case E03

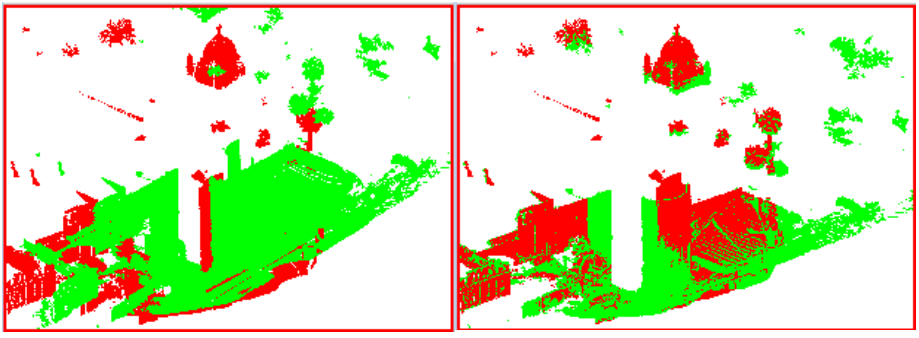

Fig. 9: the alignment of case E05

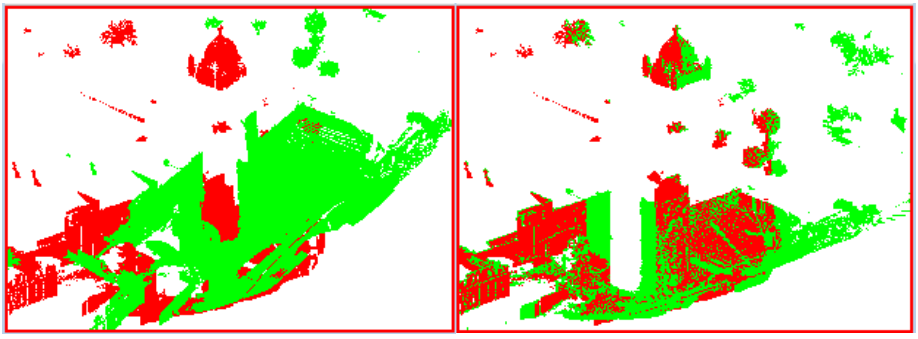

Fig. 10: the alignment of case E10

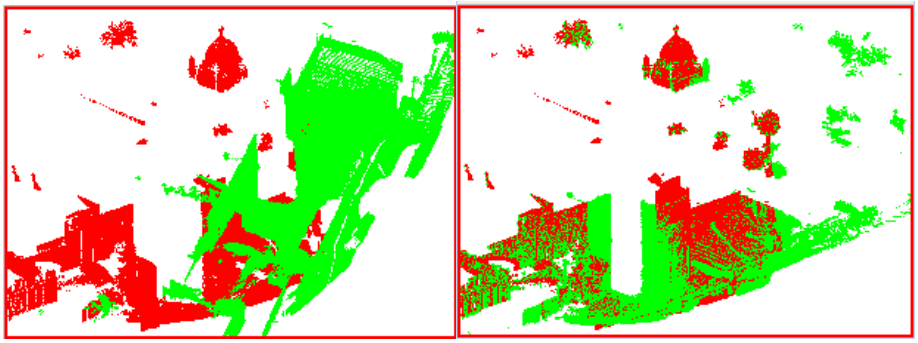

Fig. 11: the alignment of case E20

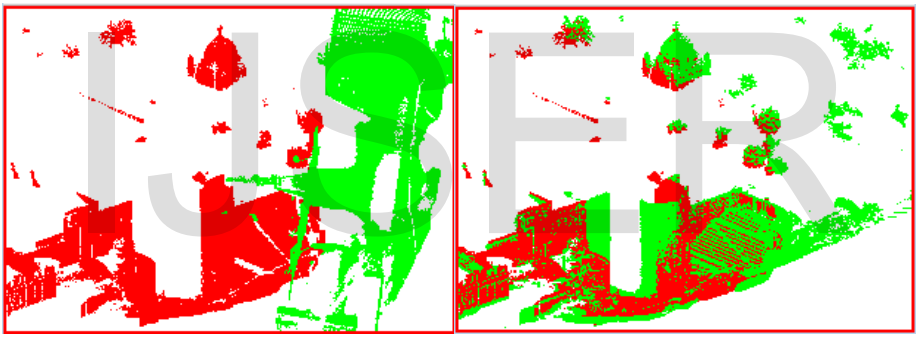

Fig. 12: the alignment of case E30

Fig.13. introduce the root mean square error (RMS) for the six cases of different target' position. The error of all cases is ranged between 0.218 to 0.222

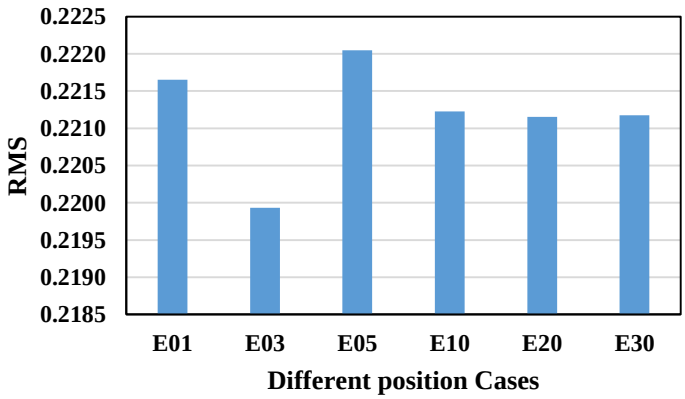

Fig. 13: the RMS error for six cases of different target' position

The algorithm was run on laptop with next specifications (Processor : Intel(R) Core(TM) i7-4702MQ Cpu @ 2.20GHz 2.19GHz , Installed memory (RAM) 8.00 GB , and System Type : 64-bit Operating system, x64-based processor with Windows edition Windows 8.1 © 2013 Microsoft Corporation System). Fig.14 shows the relation between the # No. of iteration and computation time for six cases of different target's position. It shows that when the initial target's position to the reference is near the exact solution the #no of iterations and the computation time are small while it is far #no of iterations and the computation time are irregularly high.

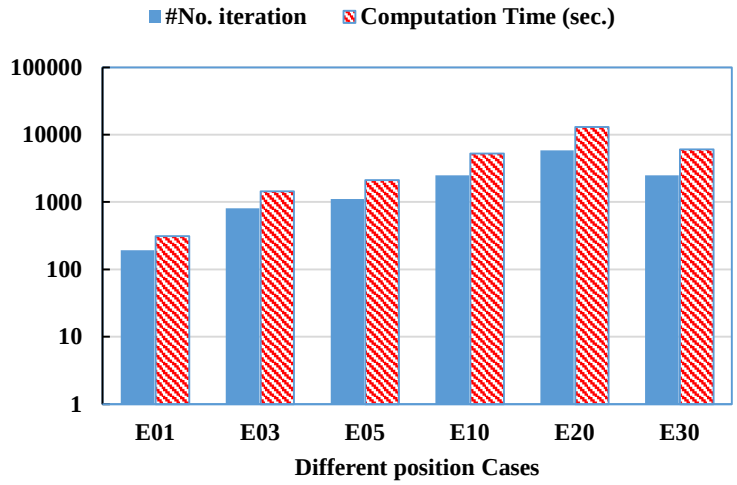

Fig. 14: The # No. of iteration and computation time for six cases of different target' position

Fig. 15 shows the change the residual which indicates the solution convergence with the #No. of iteration for six cases of different target's position. It shows that the more far the target's position there is, the slower convergence realizes.

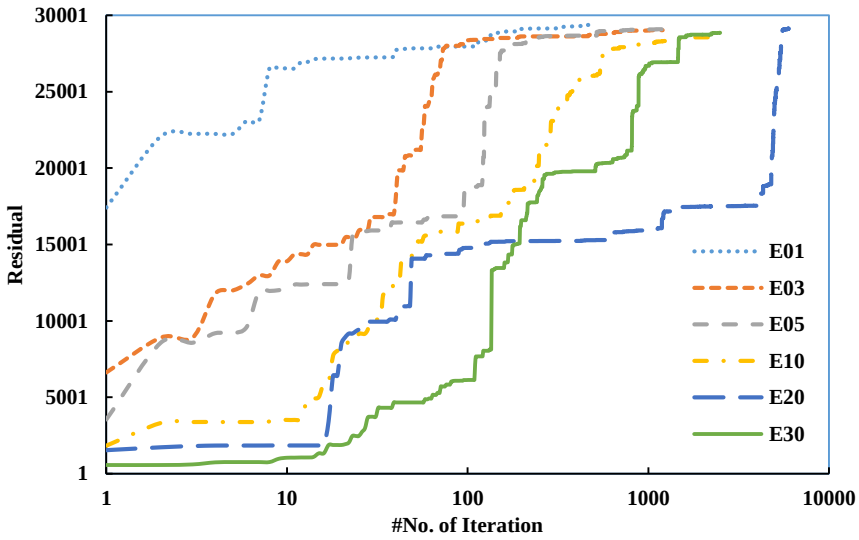

Fig. 15: The # No. of iteration versus the solution residual for six cases of different target' position

The effect of another parameter of food number in ABC method on the # No. of iteration, computation time per iteration, and the solution residual. Eight cases were taken as sample to test this effect. These cases were taken with No. of food of (5, 10, 20, 30, 40, 50, 60, and 100) and respectively denoted by

(F005, F010, F020, F030, F040, F050, F060, and F100). The all of these cases were devoted for the target' position (E20). Fig. 16 shows that the #No. of iteration as general trend decreasing with increasing of the #No. of food source while computation time per iteration increases. Fig. 17 shows that the convergence has more speed with increasing of the #No. of food source.

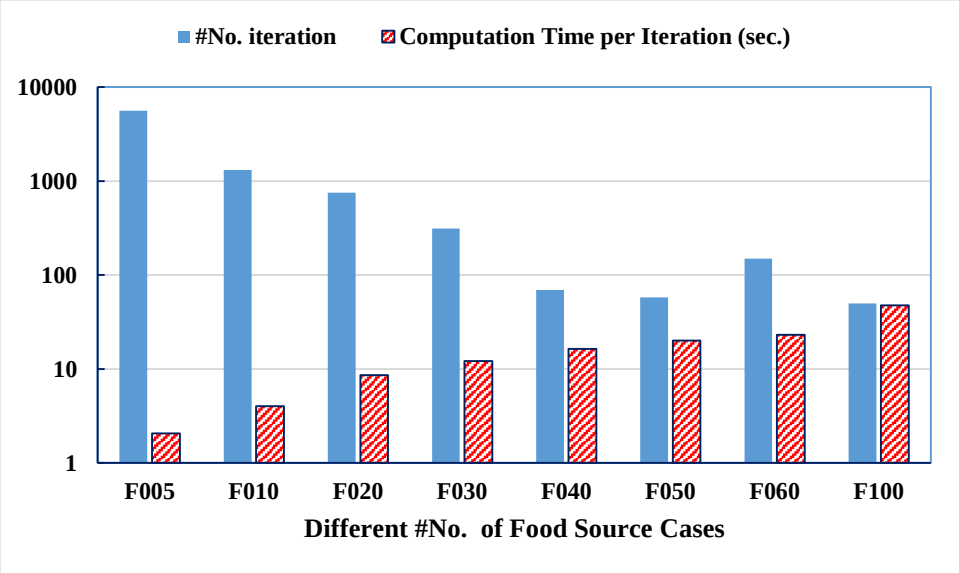

Fig. 16: The # No. of iteration and computation time of cases of different Food Number

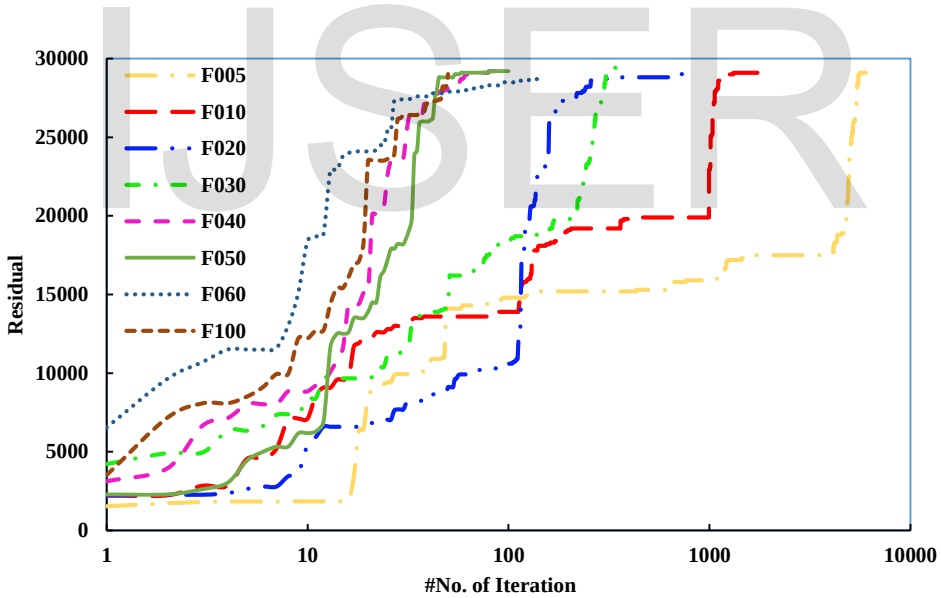

Fig. 17: The # No. of iteration versus the solution residual of cases of different Food Number

In addition, the two data sets of sphinx (Giza-Egypt) and the site of our academy (Alexandria-Egypt) were utilized to validate the proposed algorithm. The two cases is designed where the target's position is {Sol+5}. Fig's (18-19) demonstrate well-posed alignment for two cases.

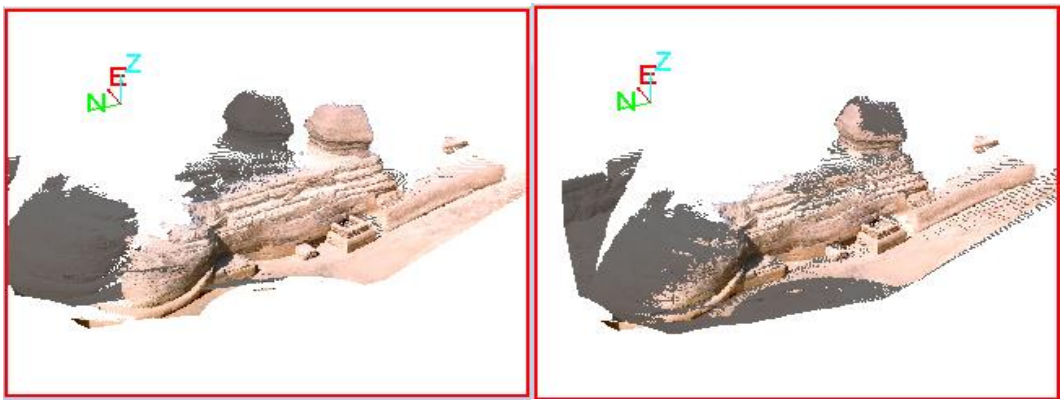

Fig. 18: The alignment of two sphinx's scenes

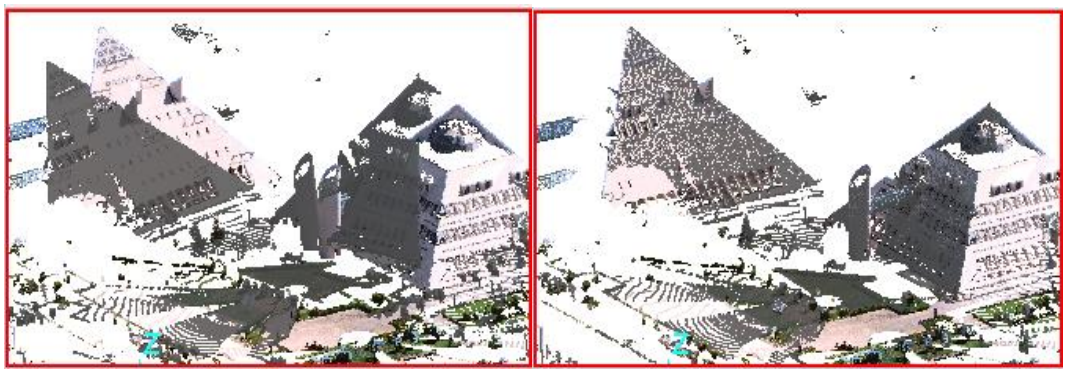

Fig. 19: the alignment of two sphinx's scenes

4. Conclusions

This research presents a new 3D laser scanner's scene registration algorithm using artificial bee colony optimization based heat kernel signature. The algorithm was tested under the change of two parameters the target's position and #No. of food source which they affect the registration accuracy and the computational time. The results demonstrate well-posed alignment for all target's positions and all #No. of food source which were listed in above-mentioned discussion. The discussion showed that #No. of iteration as general trend decreasing with increasing of the #No. of food source while computation time per iteration increases. In addition, the solution convergence has more speed with increasing of the #No. of food source. The more far the target's position there is, the slower convergence realizes.

References

[1]. C. Torre-Ferrero, José R Llata, Luciano Alonso, Sandra Robla and Esther G Sarabia. "3D Point Cloud Registration Based On A Purpose-Designed Similarity Measure", EURASIP Journal on Advances in Signal Processing a Springer open journal 2012, 2012:57

[2]. Bayumy B.A. Youssef, W.M. Sheta, M.A. Abdou "Efficient Registration of Range Images Using Wavelet Features", International Journal of Computers and Their Applications (IJCA), Vol.18, No. 2, US, June 2011

[3]. N. Meierhold, M. Spehr, A. Schilling S. Gumhold, H.-G. Maas. "Automatic Feature Matching Between Digital Images And 2D Representations Of A 3D Laser Scanner Point Cloud", International Archives of Photogrammetry, Remote Sensing and Spatial Information Sciences, Vol. XXXVIII, Part 5 Commission V Symposium, Newcastle upon Tyne, UK. 2010

[4]. C. Torre-Ferrero, S. Robla, E.G. Sarabia, J.R. Llata. "3D Registration by Using an Alternative 3D Shape Representation", Proceedings of the 7th WSEAS Int. Conf. on Signal Processing, Computational Geometry & Artificial Vision, Athens, Greece, August 24-26, 2007

[5]. Ruisheng Wang, Frank P. Ferrie, Jane Macfarlane. "Automatic Registration of Mobile LiDAR and Spherical Panoramas", Computer Vision and Pattern Recognition Workshops (CVPRW), 2012 IEEE Computer Society Conference, ISSN : 2160-7508 , 16-21 June 2012

[6]. Abbas Abedini, Michael Hahn, Farhad Samadzadegan. "An Investigation Into The Registration of Lidar Intensity Data and Aerial Images Using The Sift Approach", The International Archives of the Photogrammetry, Remote Sensing and Spatial Information Sciences. Vol. XXXVII. Part B1. Beijing 2008

[7]. Ebadat G. Parmehr, Clive S. Fraser, Chunsun Zhang, Joseph Leach. "Automatic Registration of Optical Imagery With 3D Lidar Data Using Local Combined Mutual Information", ISPRS Annals of the Photogrammetry, Remote Sensing and Spatial Information Sciences, Volume II-5/W2, 2013 , ISPRS Workshop Laser Scanning 2013, 11 – 13 November 2013, Antalya, Turkey

[8]. Yamany S.M. , Farag A.A. "Free-form surface registration using surface signatures", Computer Vision, 1999. The Proceedings of the Seventh IEEE International Conference on (Volume:2), ISBN: 0-7695-0164-8, DOI: 10.1109/ICCV.1999.790402, 20 Sep 1999-27 Sep 1999

[9]. B. Yuce , S. Packianather , E. Mastrocinque, D. Truong Pham, A. Lambiase "*Honey Bees Inspired Optimization Method: The Bees Algorithm*", Insects, ISSN 2075-4450, Vol. 4, P.p. 646-662;2013

[10]. M. Bronstein, I. Kokkinos "Scale-Invariant Heat Kernel Signatures For Non-Rigid Shape Recognition", computer vision and pattern recognition (CVPR), 2010 IEEE conference, ISSN : 1063-6919, 13-18 June 2010

[11]. Jihua Zhu, Li Zhu , Zhongyu Li, Chen Li, Jingru Cui "Automatic multi-view registration of unordered range scans without feature extraction" , Neurocomputing Vol. 171, P.p. 1444–1453 ,1 Jan. 2016

[12]. Jun Xiea, Yu-Feng Hsub, Rogerio Schmidt Ferisc, Ming-Ting Suna "Fine registration of 3D point clouds fusing structural and photometric information using an RGB-D camera", Journal of Visual Communication and Image Representation, Vol. 32, P.p. 194–204, October 2015

[13]. Dirk Holz, Sven Behnke "Registration of non-uniform density 3D laser scans for mapping with micro aerial vehicles", Robotics and Autonomous Systems, Vol. 74, Part B, , P.p. 318–330 , December 2015

[14]. G. YAN, Chuangqin LI "An Effective Refinement Artificial Bee Colony Optimization Algorithm Based On Chaotic Search and Application for PID Control Tuning", Journal of Computational Information Systems 7: 9 (2011) 3309-3316

[15]. A. L. Bolaji, A. T. Khader, M. A. Al-Betar, M. A. Awadallah "Artificial Bee Colony Algorithm, Its Variants And Applications: A Survey", Journal of Theoretical and Applied Information Technology, Vol. 47, No.2 , 20th January 2013.